Available online at www.sciencedirect.com

ScienceDirect

Energy Procedia 84 (2015) 8 – 16

Energy Procedia

E-MRS Spring Meeting 2015 Symposium C - Advanced inorganic materials and structures for photovoltaics

Assessment of chemical and electronic surface properties of the $Cu_2ZnSn(SSe)_4$ after different etching procedures by synchrotron-based spectroscopies.

Tetiana Olar[a]*, Iver Lauermann[a], Haibing Xie[b], Markus Neuschitzer[b], Edgardo Saucedo[b], Wolfram Calvet[a], Alexander Steigert[a], Bünyamin Ümsür[a], Binoy Chacko[a], Vladimir Parvan[a], Mihaela Gorgoi[a], Boris Senkovskiy[c] and Martha Ch. Lux-Steiner[a]

[a]*Helmholtz-Zentrum Berlin für Materialien und Energie GmbH,Albert-Einstein-Str. 15, 12489 Berlin,Germany*
[b]*Catalonia institute for Energy Research- IREC, Jadinsde les Dones de Negre 1, 08930 Sant Adrià de Besòs (Barcelona), Spain*
[c]*Institute of Solid State Physics, Dresden University of Technology, 01062 Dresden, Germany*

Abstract

Kesterite $Cu_2ZnSn(S,Se)_4$ absorber layers with different [S]/([S]+[Se]) ratios were studied using XPS, UPS, Hard X-ray (HIKE) photoemission and the Near Edge X-ray Absorption Fine Structure spectroscopy (NEXAFS). The samples were prepared by IREC using sequentially sputtered metallic precursor stacks with metal ratios of [Cu]/([Zn]+[Sn])=0.80, [Zn]/[Sn]=1.20 followed by annealing under S+Se+Sn atmosphere. Different etching procedures were used depending on the sample´s composition. It is shown that the surface composition varies from that of the bulk, especially for the Se-rich samples. Contamination with sulfur is detected after using a Na_2S etching solution for the pure Se kesterite. A Cu-depleted surface was found for all samples before and after etching. HIKE measurements show a higher [Zn]/[Sn] ratio in the near surface region than on the very surface. This is explained by the fact, the etching procedure removes secondary phases from the very few surface layers, while some of ZnS(e) is still buried underneath. In order to investigate the band gap transition from the pure sulfide (1.5 eV) to the pure selenide (1 eV), the valence and conduction band of the respective absorbers were probed. According to UPS and HIKE measurements, the relative distance between Fermi level (E_f) and valance band maximum (VBM) for sulfide sample was 130 meV larger than for selenide. Using NEXAFS on the copper, zinc and tin edges, the development of the conduction band with increasing [S]/([S]+[Se]) ratios was studied. Stoichiometric powder samples were used as

* Corresponding author. Tel.: +49-30-806215693; fax: +49-30-806215752.
E-mail address: tetiana.olar@helmholtz-berlin.de

Peer-review under responsibility of The European Materials Research Society (E-MRS)
doi:10.1016/j.egypro.2015.12.289

reference materials.

Peer-review under responsibility of The European Materials Research Society (E-MRS)

Keywords: kesterite, thin-film solar cells, x-ray photoelectron spectroscopy, chemical etching, surfaces, heterojunction, absorption spectroscopy, band offsets.

1. Introduction

The kesterite material $Cu_2ZnSn(S,Se)_4$ (CZTSSe) is a promising candidate for application in PV due to its earth-abundant and nontoxic constitutes. It can be obtained by replacing In and/or Ga with Zn and Sn in $Cu(In,Ga)(S,Se)_4$ (CIGSSe). The current record efficiency for CZTSSe (12.7%) is still far below that of CIGSSe (21.7%). One of possible reasons can be a high recombination rate at the absorber/buffer interface and a resulting deficit in the V_{oc}.[1],[2]. For the further optimization of the thin-film solar cells a detailed study of the chemical and electronic properties of the respective absorber material is necessary. Therefore, we have used a wide range of X-ray based spectroscopies, such as standards X-ray Photoelectron (XPS) and Hard X-ray (HIKE) Photoelectron Spectroscopies in order to investigate the surface structure of kesterites with different [S]/([S]+[Se]) ratios before and after chemical etchings and compared them with the bulk concentrations. Using Ultraviolet Photoelectron Spectroscopy (UPS) and Near Edge X-ray Absorption Fine Structure (NEXAFS) we have determined valance band maximum (VBM) and conduction band minimum (CBM) offsets for the mentioned kesterite samples to concentrate on heterojunction formation and possible routes of devices improvement.

2. Surface vs. bulk composition of Cu2ZnSn(S,Se)4 with different [S]/([S]+[Se]) ratios

$Cu_2ZnSn(S,Se)_4$ samples with different [S]/([S]+[Se]) ratios (~1,5 µm thick) were produced by reactive thermal annealing of metallic precursor stacks [3],[4]. A sequence of metal layers Cu/Sn/Cu/Zn was deposited by magnetron sputtering onto a Mo-coated soda-lime glass. The precursors were reactively annealed in a tubular furnace in a graphite box in the presence of solid S and/or Se and Sn. Therefore, the entire range of [S]/([S]+[Se]) ratios between a pure sulfide and a pure selenide is covered and the sample numbers and their composition are shown in Table 1.

Table 1. Kesterite samples with different [S]/([S]+[Se]) ratios. The number of the sample will be used throughout this document. The cation composition is identical for all samples

Number	Precursor		Absorber comp. by EDX			Etching
	Cu/(Zn+Sn)	Zn/Sn	Cu/(Zn+Sn)	Zn/Sn	S/(S+Se)	
1	0.8	0.2	0.84	1.18	1	$HCl+(NH_4)_2S$
2			0.87	1.22	0.95	$HCl+(NH_4)_2S$
3			0.87	1.27	0.64	$HCl+(NH_4)_2S$
4			0.89	1.32	0.49	$(NH_4)_2S$
5			0.85	1.17	0.24	$(NH_4)_2S$
6			0.82	1.16	0.06	$(NH_4)_2S$
7			0.81	1.09	0	$KMnO_4/H_2SO_4+Na_2S$

2.1. Influence of etching

In order to remove unwanted secondary phases from the surface of the CZTS(e) absorbers, different chemical etchings have been developed depending on the absorber composition (see Table 1). Thus, a $HCl+(NH_4)_2S$ solution

was used for CZTS and S-rich CZTSe to remove ZnS and $Sn_x(Se,S)$ secondary phases (5min 5% v/v HCl aqueous solution, $(NH_4)_2S$ 22% v/v aqueous solution for 1 min) [5],[6]. Se-rich absorbers were etched with a $(NH_4)_2S$ solution, as in a previous case [6],[4]. Pure Se-based CZTSe was etched with $KMnO_4/H_2SO_4$ followed by a Na_2S-solutions, which removes unwanted ZnSe phases [7].

After the wet chemical etching in the laboratory facilities, samples were put under the vacuum of the experimental set up to perform X-ray based experiments. The transfer of the samples was unavoidably connected with contamination of the sample surface. The air exposure of the CZTS(e) samples was minimized to the 2-3min. Nevertheless, several monolayers of oxidized compounds, formed on the very top of the sample´s surface, contribute to the final photoemission signal and were taken into account during the data evaluation.

The surface of the samples was examined before and after etchings with XPS and UPS in ultra-high vacuum ($<8{,}5\times10^{-9}$ mbar) using Al Kα (1486,6 eV) and He I (21,2 eV) excitations respectively. A CLAM4 electron spectrometer (Thermo VG Scientific), calibrated according to [8], was used. The XPS survey spectra (not shown) of as-received samples are dominated by kesterite-related photoemission and Auger peaks, as well as by prominent signals from C, O and Na. After chemical etchings, the O- and C-related photoemission line intensities decrease drastically and Na is almost completely gone. On the other hand, signals from Cu, Zn, Sn, S and/or Se become more pronounced and can be used for the further analyses of the chemical structure of sample surfaces.

The main difference between the seven samples is in the sulphur and selenium content, the bulk concentrations of which were initially measured with EDX (Table 1). We analysed the detailed selenium 3p and sulphur 2p peaks in order to obtain the surface [S]/([S]+[Se]) ratios before and after etching and compared them with those obtained from the bulk data. A quantitative evaluation of the peaks mentioned above was done in several steps: after background subtraction, peaks were fitted with a set of Voigt functions, normalised with photoionization cross sections from [9],[10],[11], with the calculated mean free path using the QUASES-IMFP-TPP2M code, Version 2.2 taken from [12] and with the transmission function of our electron analyser.

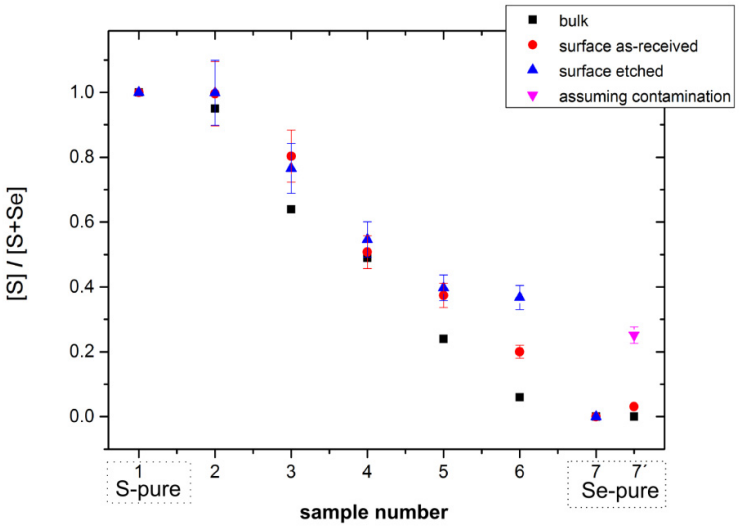

Fig. 1. [S]/([S]+[Se]) ratios on as-received and etched surfaces. EDX data is shown as bulk. For sample 7, a second fitting procedure was used, assuming a sulfur contamination, resulting in two different results 7 and 7' (see text).

In Figure 1 the [S]/([S]+[Se]) ratios derived from the XPS data before and after etching is plotted together with EDX bulk data; which is supposed to be the same after superficial etching of a few thin surface layers. Here, pure

sulfide and selenide samples are shown as 1 and 0, respectively. Samples 2 and 4 show good agreement between bulk and surface compositions, while samples 3, 5 and 6 seem to have a higher S content on the surface. In case of the Se-rich sample, the [S]/([S]+[Se]) ratio increases considerably after etching, probably because the $(NH_4)_2S$ solution has removed Sn_xSe from the surface.

Sample number 7, a pure selenide kesterite, seems to have an S contamination on the surface after the chemical etching step (denoted 7´in Fig.1). This became clear after several attempts to fit Se 3p peak of the etched surface. The residual intensity at the binding energy, which is typical for the S 2p peak, remained uncovered, even if several sets of selenium doublets were used. The origin of the sulphur contamination can be a final Na_2S etching step, when S atoms could be incorporated into the surface. It is also possible that the contamination occurred during a subsequent handling of the precursors, namely during a reactive annealing in the furnace that had some sulphur traces.

For the further investigation of [$KMnO_4/H_2SO_4$ + Na_2S] etching of the Se-pure kesterite, we examined the cation composition of the two identical CZTSe samples after two different etching procedures, namely the recommended [$KMnO_4/H_2SO_4$ + Na_2S] etch and the well-established KCN solution. After XPS examination of the etched surfaces, the relative cation ratio was calculated and the obtained results are depicted in Figure 2. The deviation in composition of the two initially identical samples became clear: the Zn content on the CZTSe surface after the complex oxidation etching is much lower than that of the KCN etched CZTSe sample and similar to the Zn concentration on the surface of the CZTS sample. Therefore, etching with a solution containing potassium permanganate in sulphuric acid provides a more Zn-poor CZTSe surface, in comparison to the KCN etching step.

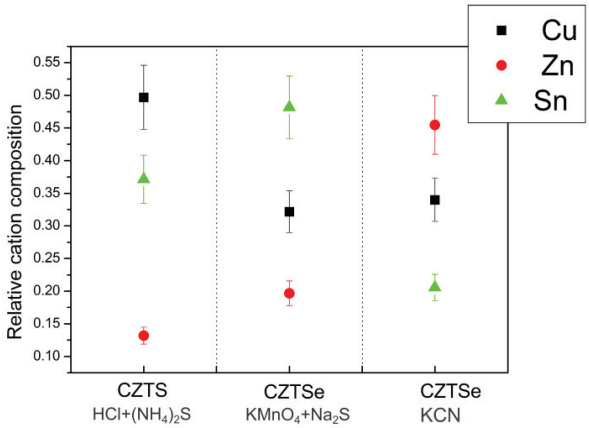

Fig. 2. Relative cation composition of the CZTS(e) absorber samples after applied etchings.

2.2. High energy XPS

In order to have a further look into surface composition, high energy XPS measurements were performed at the KMC-1 beamline at the electron storage ring BESSY II Berlin (Germany).[14] The high kinetic energy end station (HIKE) allows to tune excitation the energy (E_{ex}) of the X-ray beam from 2.01 keV up to 12 keV and therefore to increase the information depth from roughly 5 nm up to 25 nm.

The surface chemical compositions of the S-rich samples 2 and 3 were measured using different excitation energies and the obtained cation ratios were compared to the bulk value and presented in Figure 3. Both samples show similar behavior: the ratio [Zn]/[Sn] measured at relatively low excitation energies is less than that of measured at higher energies. One could speculate that the applied chemical etching removed ZnS just from the very

few surface layers, while some unwanted secondary phases are still buried deeper in the near-surface region, within the information depth of the HIKE.

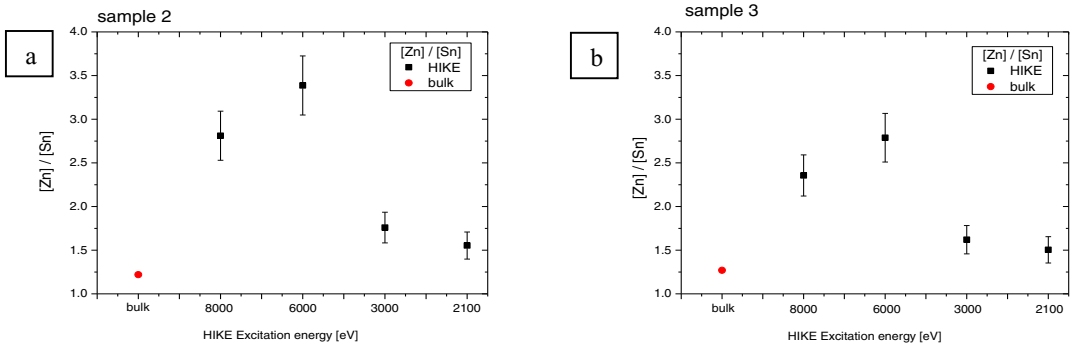

Fig. 3. Comparison of the relative [Zn]/[Sn] ratios measured on sample (a) 2 and (b)on sample 3 with different excitation energies HIKE with EDX-derived data.

3. Determination of the valance band maxima for CZTS and CZTSe

The optical band gaps of kesterites are well known and reported to be E_g=1 eV for the Se-pure and E_g=1,5 eV for the S-pure compounds. [15],[16] The difference ΔEg=0.5 eV when going from CZTSe to CZTS causes changes in the band alignment on the absorber/buffer interface, which are crucial for the device performance. And according to theoretical calculations [15], the change in the band gap of the semiconductor induces shifts in both, valance and conduction bands respectively. The difference of 0,5 eV would be distributed as 0,15 eV shift of valance band maximum (VBM) and 0,35 eV shift of conduction band maximum (CBM) of the respective absorbers.

In order to find experimental proof for these calculations, we measured the VBM of 7 kesterite samples with different [S]/([S]+[Se]) ratios as described above, with a laboratory UPS source (excitation energy E_{ex}=21,2 eV) [13] and synchrotron –based radiation with E_{ex} varying from 80 eV up to 2100 eV. A set of 7 UPS spectra, referenced to the gold Fermi level, is shown in Figure 4. The linear extrapolation (black solid lines) of the leading edges of the spectra is used to determine the VBM for each absorber composition with an error margin of 100 meV.

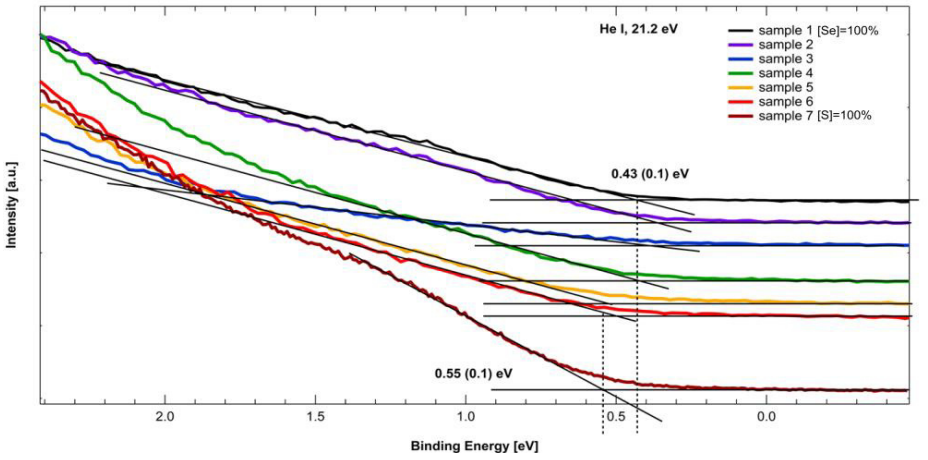

Fig. 4. UPS spectra of the investigated kesterite samples with different [S]/([S]+[Se]) ratios. The linear extrapolation of the leading edge of the valance band edge curves is extrapolated until the baseline. The point of intersection is used as VBM value.

The determined VBM values using the He I excitation revealed a shift of 0,13eV from 0,43±0,1 eV for the pure selenide to 0,55±0,1 eV for the pure sulfide kesterite samples. This finding is consistent with measurements done at the synchrotron at different excitation energies. Corresponding VBM shifts are shown in Table 2. Only a slight deviation of ±0,02 eV was found when E_{ex}=1300 eV was used (ΔVBM=0,15 eV), which is in a good agreement with laboratory experiment and previously reported data [17].

Table 2. Relative VBM shift measured at different excitation energies.

Excitation energy (eV)	Relative VBM shift (eV)
21,1	0.13±0.1
80	0.05±0.1
600	0.13±0.1
1000	0.12±0.1
1300	0.15±0.1
2100	0.13±0.1

However, it is possible to see that the VBM shift at Eex =80 eV didn't reveal a distinct shift and there are several possible reasons why. First, if we refer to the universal curve of a mean free path of photoelectrons in matter vs applied excitation energy [21], we would notice that it has its experimentally derived minimum at around of 80 eV. Measurements at this energy became extremely surface sensitive and cannot draw a comprehensive experimental picture. Second, this extremely small value of VBM shift could be due to a measurement or sample preparation error, when the specimen transfer to other experimental end-stations was done.

4. Determination of the conduction band minimum for CZTS and CZTSe

It was already mentioned that the conduction offset at the heterojunction plays an important role for the thin film solar cell performance. We have determined the distance between Fermi level and VBM for the kesterite samples with the change of the [S]/([S]+[Se])-ratio. However, the CBM position relative to the Fermi level is more difficult to obtain. The most common method for that purpose is inverse photoelectron spectroscopy (IPES).[18] Unfortunately, we didn't have a possibility to use IPES for our measurements, therefore Near Edge X-ray Absorption Fine Structure (NEXAFS) was chosen as an alternative tool to probe CBM.[19] However, NEXAFS has some unresolved difficulties [19] such as spectrum broadening, possible formation of excitons leading to shifts of the measured absorption edges, and quantum mechanics restrictions, namely the dipole selection rule Δl=±1, where 1 is the azimuthal quantum number. Carefully interpreted NEXAFS data nevertheless can provide a reliable sought-for relative CBM to E_f distance of the particular semiconductor.

The position of the absorption edge provides the energy difference between the probed core level and the first allowed unoccupied state in the conduction band. Besides that, NEXAFS is very sensitive to the chemical environment of the probed atom, in some cases more that XPS, for instance, and can be used to investigate an element in the a specific phase [19].

Therefore, as the impinging beam energy is increasing, the core level electrons are getting excited into the final state in the conduction band, leaving behind a core hole after the absorption. Thus, we assume that the unexcited state, prior to X-ray absorption, is an initial state, and a core hole represents a final state of the studied system. This means, that NEXAFS shows the density of unoccupied states in the conduction band in the ground state, before the absorption occurred, i.e. NEXAFS spectra contain information about the local density of states (LDOS) seen by the excited atom in the initial state.[19] Experimental data supported with LDOS calculations can be used to determine the position of the conduction band.

However, the straightforward interpretation of the absolute position of the absorption edge is not possible, not only because of distortions cause by the core hole (i.e. the final state), but it also can happen, that the LDOS measured by NEXAFS does not overlap with the bottom of the conduction band, as we expected.

Now to focus on the experiment in detail, it is necessary to say the energy that is released after filling a created hole can be dissipated through different mechanisms such as fluorescence or the emission of Auger electrons, giving a possibility to study absorption in different detection modes. In this work, the fluorescence mode was used, due to samples and instrument configurations and further, we will focus mainly on two out of seven samples, namely pure S (number 1) and pure Se (number 7). A typical NEXAFS spectrum, shown in Figure 5, contains the absorption edge itself and a region of tens of eV just after the edge, and is therefore called *near edge* fine structure spectroscopy. When the opening of the band gap is studied, such as in this work, calibrated NEXAFS spectra obtained from different samples can be used to determine a relative CBM shift, like in Fig.5, where the Cu L_3 edge of CZTS sample is shown together with the CZTSe Cu L_3 edge. Detailed XPS spectra of Cu $2p_{3/2}$ didn't reveal a shift of binding energies when going from CZTS to CZTSe, thus the corresponding Cu L_3 absorption edges positions represent a real energy difference between the core levels and the final states of electrons in the conduction band.

A shift of 0,3±0,1 eV for the Cu L_3 edges was determined using the linear extrapolation of the leading edge of the spectra to the baseline. The latter behaviour, i.e. a shift of 0,35±0,1 eV, is also observed for the Zn L_3 edge (not shown), reproducing the found CB shift when the band gap is increasing from 1eV of CZTSe to 1,5 eV for CZTS. However, the Sn L_3 absorption edge (Fig. 5 (b)), didn't reveal a similar shift, as well as other edges of this element, M_5 and M_3 (see Table 3). It becomes clear that in order to understand the evolution of electronic structure of kesterites several absorption edges need to be measured.

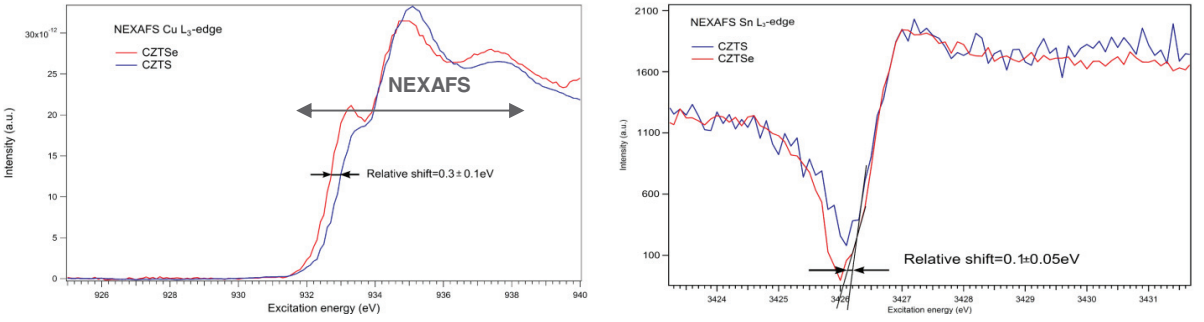

Fig. 5. Absorption edges of Cu L_3, Sn L_3 from CZTS (blue) and CZTSe (red) samples measured in fluorescence mode. The energy scale is not absolute, but the positions of the edges are relatively correct to each other, thus the shift in spectra can be used as a real energy different in CBM positions.

Table 3 summarizes different experiments that have been done at the BESSY II synchrotron in Berlin, Germany, using the tender x-ray KMC-1 beam line (2keV to 12keV) with the HIKE end station, with a Bruker fluorescence detector, at the soft x-ray Russian-German Beam Line and at the soft x-ray U492PGM1 beam line using the CISSY end station.

Table 3. Relative absorption edge shift measured at different end station: RGBL, CISSY and HIKE.

Absorption edge	Relative shift (eV)
Cu L_3 RGBL	0.3±0.1
Cu L_3 CISSY	0.25±0.1
Zn L_3 RGBL	0.35±0.1
Sn M_5 RGBL	0.1±0.1
Sn M_3 RGBL	0.1±0.1
Sn L_3 HIKE	0.1±0.1

Therefore, the found shift for the Cu L_3 and Zn L_3 edges are in well agreement with theoretically predicted shifts of the conduction band minimum, described in the section 3. The calculations of the Repins. et al.[15] forecast the changes in the CBM caused with different [S]/[S+Se] ratio, namely the shift of 0,35 eV relatively to Fermi level. However, despite the findings for the Cu and Zn-related spectra, the shift in the absorption spectra of Sn didn't show values in the same range.

There could be several reasons for such uncertainty in the shifts of the different absorption edges. First, the stoichiometry of pure sulphur and selenium compounds are different. This factor can be studied in details with X-ray diffraction in future.

Secondly, the LDOS of each of the studied groups of atoms may contribute differently into conduction band bottom; therefore, the transition studied with NEXAFS also would be different. The measured energy distance between core level and final state in the CB is elemental specific and can vary or not within the given stoichiometry of the sample. The local electronic environment of each atom of the material with the fixed composition and the measurable optical band gap became finally evident at the macroscopic level.[19] Theoretical modelling of the unoccupied states in the CB is required to gain more an insight into this problem.

To complete the picture, we refer to the initial and the final states definitions. XPS initial and final states are the same as defined for NEXAFS, which makes it possible to compare XPS- and NEXAFS-derived data. However, another uncertainty, that possibly influences the results of the experiment, is that the laboratory XPS is a surface sensitive technique, with the information depth of 3-5 nm, as well as UPS, used to determine VBM, while NEXAFS detected in a fluorescence mode is considered to be a more bulk sensitive method (300-400 nm).

5. Conclusion

In summary, we have studied 7 kesterite samples with identical metal concentration, but with different [S]/([S]+[Se]) ratios, ranging from 0 (pure selenide) to 1 (pure sulfide). We compared their surface chemical compositions with known bulk values before and after applied etchings. It was shown that as-received surfaces differ from the expected stoichiometry and change even more after applying complex oxidation etching procedures.

The valance band maxima of the absorbers were measured at different excitation energies, in order to cover a wide range of the information depth in the material. A reproducible shift of 0,13±0,1eV was found when going from CZTSe to CZTS compound. NEXAFS was used as tool to the probe conduction band minimum of the semiconductors. A relative shift of CBM of 0,3±0,1eV was detected, using several absorption edges. Presented results can be used to tailor electronic and chemical surface properties of kesterites with different [S]/([S]+[Se]) ratios to improve final thin-film solar cells devices.

Acknowledgements

The research leading to these results has received funding from the People Program (MarieCurieActions) of the European Union's Seventh Framework Program FP7/2007-2013/ under REA grant agreement no. 316488 (KESTCELLS) and by European Regional Development Founds (ERDF, FEDER Programa Competitivitat de Catalunya 2007–2013). Authors from IREC belong to the M-2E (Electronic Materials for Energy) Consolidated Research Group and the XaRMAE Network of Excellence on Materials for Energy of the "Generalitat de Catalunya". H. Xie thanks the "China Scholarship Council" fellowship (CSCno.201206340113), and E.S. the MINECO, Spain for the "Ramon y Cajal" fellowship (RYC-2011-09212). The authors thank the Helmholtz-Association for the financial support.

References

[1]. Kim J, Hiroi H, Todorov TK, Gunawan O, Kuwahara M, Gokmen T, Hopstaken M, Shin B, Lee YS, Wang W, Sugimoto H, Mitzi BD. High efficiency Cu2ZnSn(S,Se)4 solar cells by applying a double In2S3/CdS emitter. Adv. Mater. 2014, 26, 7427.

[2]. ZSW, Baden-Württemberg, Stuttgart, Germany, http://www.zsw-bw.de/uploads/media/pr12-2014-ZSW-WorldrecordCIGS.pdf (accessed:Dec. 2014).

[3]. Fairbrother A, Fontané X, Izquierdo-Roca V, Espindola-Rodriguez M, López-Marino S, Placidi M, Juan López-García, Pérez-Rodríguez A, Saucedo E. Single-Step Sulfo-Selenization Method to Synthesize Cu2ZnSn(SySe1−y)4 Absorbers from Metallic Stack Precursors. ChemPhysChem. 2013, 14, 1836-1843.

[4]. Xie H, Dimitrievska M, Fontané X, Sánchez Y, López-Marino S, Izquierdo-Roca V, Bermúdez V, Pérez-Rodríguez A, Saucedo E. Formation and impact of secondary phases in Cu-poor Zn-rich Cu2ZnSn($S_{1-y}Se_y$)4($0 \leq y \leq 1$) based solar cells. Solar Energy Materials & Solar Cells. 2015, 140, 289–298.

[5]. Fairbrother A, García-Hemme E, Izquierdo-Roca V, Fontané X, Pulgarín-Agudelo FA, Vigil-Galán O, Peérez-Rodríguez A, Saucedo E. Development of a selective chemical etch to improve the conversión efficiency of Zn-rich Cu2ZnSnS4 solar cells. J.Am.Chem.Soc. 2012, 134, 8018–8021.

[6]. Xie H, Sánchez Y, López-Marino S, Espíndola-Rodríguez M, López-García J, Neuschitzer M, Sylla D, Fairbrother A, Pérez-Rodríguez A, Sauced E. Impact of Sn(S,Se) secondary phases in Cu2ZnSn(S,Se)4 solar cells: a chemical route for their selective removal and absorber Surface passivation. ACS Appl. Mater. Interfaces. 2014, 6, 12744–12751.

[7]. Lopez-Marino S ,Sanchez Y, Placidi M, Fairbrother A, Espindola-Rodriguez M, Fontane X, Izquierdo-Roca V, Lopez-Garcia J, Calvo-Barrio L, Perez-Rodriguez A, Saucedo E. ZnSe Etching of Zn-rich Cu2ZnSnSe4: an oxidation route for improved solar-cell efficiency. Chem. A Eur. J. 2013, 19 (44), 14814–14822.

[8]. Briggs D, Seah MP (eds.). Practical Surface Analysis. John Wiley & Sons.1990, Vol. 1.

[9]. Scofield JH. Hartree-Slater Subshell photoionization cross-sections at 1254 and 1487 eV. J. Electron Spectrosc. Relat. Phenom.1976, 8, 129.

[10]. Trzhaskovskaya M B, Nikulin V K, Nefedov V I, Yarzhemsky V G. Non-dipole second order parameters of the photoelectron angular distribution for elements Z = 1–100 in the photoelectron energy range 1–10 keV. Atomic Data and Nuclear Data Tables. 2006, 92:245.

[11]. Yeh J J, Lindau I. Atomic Data and Nuclear Data Tables. 1985, 32, 1.

[12]. http://www.quases.com/.

[13]. Ruckh M, Schmid D, Schock H W. Photoemission studies of the ZnO/CdS interface. Appl. Phys.1994, 76, 5945-5948.

[14]. Schäfers F, Mertin M, Gorgoi M, KMC-1: A high resolution and high flux soft x-ray beamline at BESSY. Rev of Sci Instr 2007;78:123102.

[15]. Repins I, Vora N, Beall C, Wei S, Yan Y, Romero M, Teeter G, Du H, To B, Young M, Noufi R, Kesterites and Chalcopyrites: A Comparison of Close Cousins, Preprint: Presented at the 2011 Materials Research Society Spring Meeting San Francisco, California April 25–29, 2011.

[16]. Chen S, Walsh A, Yang J H, Gong X G, Sun L, Yang P X, Chu J H, Wei S H. Compositional dependence of structural and electronic properties of Cu2ZnSn(S,Se)4 alloys for thin film solar cells. Phys. Rev. 2011, B 83, 125201.

[17]. Haight R, Barkhouse A, Gunawan O, Shin B, Copel M, Hopstaken M, Mitzi D B. Band alignment at the Cu2ZnSn(SxSe1−x)4 /CdS interface. Appl Phys Lett. 2011, 98, 253502.

[18]. Fischer Ch H, Bär M, Glatzel Th, Lauermann I, Lux-Steiner M C. Interface engineering in chalcopyrite thin film solar devices. Sol.Energy Mater. Sol.Cells. 2006, 90, 1471–1485.

[19]. Johnson B, Klaer J, Merdes S, Gorgoi M, Höpfner B, Vollmer A, Lauermann I. Limitations of Near Edge X-ray Absorption Fine Structure as a tool for observing conduction bands in chalcopyrite solar cell heterojunctions. J. Electron Spectrosc. Relat. Phenom. 2013, 190, 42–46.

[20]. Sarmiento-Perez R, Botti S, Schnohr C S, Lauermann I, Rubio A, Johnson B. Local versus global electronic properties of chalcopyrite alloys: X-ray absorption spectroscopy and ab initio calculations. Jpn. J. Appl. Phys. 2014, 116, 093703.

[21]. Briggs D, Seah M P. Practical Surface Analysis . 1990, Wiley, Chichester, pp. 85-141, 2nd edn.